Supplemental Figure 1. Icmt deficiency affects neither the endocrine pancreas nor pancreatic development. (A) Glucose tolerance tests (left panel) were carried out on female (F) and male (M) mice of the indicated genotypes that also carried a *PDX-1-Cre* allele. No significant difference in the area under the curve (AUC) was detected (right panel). (B) Representative H&E stained sections of pancreata from 25 month old mice of the indicated genotypes. Bars indicate 100 μm. (C) *Icmt*$^{flx/+}$;*PDX-1-Cre* and *Icmt*$^{flx/flx}$;*PDX-1-Cre* mice were crossed with animals harboring an *LSL-lacZ* transgene expressed from the *ROSA26* locus to yield the indicated genotypes. Shown are frozen sections of pancreata from 10 week old mice treated with X-gal to stain cells that express β-galactosidase (blue) and counterstained with eosin (red). Whereas almost all visible pancreatic cells stained blue in sections from *Icmt*$^{flx/+}$;*PDX-1-Cre;ROSA26-LSL-LacZ* pancreata, some β-galactosidase negative cells can be seen in pancreata from *Icmt*$^{flx/flx}$;*PDX-1-Cre;ROSA26-LSL-LacZ* mice (arrow). Blue cells indicate that Icmt deficient cells contribute to the developing pancreatic tissue. Non-pancreatic tissues, such as blood vessels (arrowhead) and lymph nodes, are β-galactosidase negative. Bars indicate 500 μm. (D) Icmt enzymatic activity in membrane fractions of pancreatic homogenates from 10 week old mice of the indicated genotypes. Data shown are mean ± SEM, n=3, $p<0.05$.

Supplemental Figure 2. Icmt deficiency does not cause pancreatic neoplasia in the absence of oncogenic K-Ras even when p53 is inactivated. Representative H&E stained paraffin sections are shown of pancreata of 12 month old mice with the indicated genotypes. No PanINs or other pathology were found in the pancreata of either genotype. Bars represent 100 μm.

Supplemental Figure 3. Icmt deficiency results in more extensive PanIN lesions and fibrosis in *PDX-1-Cre;LSL-KRAS^{G12D}* mice. (A) Sections of Pancreas from mice of the indicated genotypes were stained with Alcian Blue to visualize the mucin content characteristic of PanIN lesions. Right panel shows plots of the mean percent area of Alcian Blue staining in 5 fields of view. Bars represent 100 μm. Data shown are mean ± SEM of sections taken from 6 pairs of littermate mice $p<0.05$. (B) Sections of pancreas from 3 month old mice of the indicated genotypes were stained by IHC for α-smooth muscle actin.

Supplemental Figure 4. Icmt is not required for Ras activity and signaling. (A) GST-RBD pulldown of GTP loaded Ras in lysates of HeLa cells ±*ICMT* knockdown stimulated with 10 ng/ml of EGF for 3 min. Cells were transfected with siRNA targeting *ICMT* or a non-targeting siRNA 72 hrs before lysis. Data shown are mean ± SEM (n=3). (B) Immunoblots for total Erk (tErk), phospho-Erk (pErk), and Icmt in lysates of HeLa cells transfected with either siRNA targeting *ICMT* or non-targeting (NT) siRNA for 72 hrs, or dominant negative GFP-H-Ras17N for 24 hrs then stimulated with 5 ng/ml of EGF for the indicated times before lysis. The amount of pERK/tErk for each condition was normalized to the maximum stimulation for each experiment. Data shown are mean ± SEM (n=4). (C) *in vitro* Icmt activity towards *N*-acetyl-*S*-farnesyl-L-cysteine of 10 μg of a total membrane fraction isolated from HeLa cells that had been transfected with either siRNA targeting *ICMT* or non-targeting siRNA for 72 hrs.

Supplemental Figure 5. Icmt deficiency does not affect cerulein-induced acute or chronic pancreatitis. (A) H&E stained paraffin sections of pancreata of 3 month old mice of the indicated genotypes in which acute pancreatitis was induced by cerulein as described in

Experimental Procedures. Sections from pancreata on days 0, 3 and 7 relative to the cessation of cerulein are shown. Differences among genotypes were observed neither in the extent of inflammation (scored as interstitial infiltrates within acinar tissue) nor in the rate or extent of recovery. (B) H&E stains of pancreata from the indicated genotypes after induction of chronic pancreatitis as described in Experimental Procedures showing no apparent differences. Bars indicate 100 μm.

Supplemental Figure 6. Ste14 deficiency inhibits Notch1 signaling in *D. melanogaster* wing development. Adult wings of *D. melanogaster* transgenic for *UAS-shSte14*, a GAL4 responsive hairpin that silences *Icmt*. GAL4 expression was driven with a wing-specific promoter (*MS1069-GAL4*). Icmt deficiency in the developing wing phenocopies the terminal vein bifurcation (arrows) observed in the wings of *Delta* (Dl) flies that are deficient for the Notch ligand.

Supplemental Figure 7. Ste14 deficiency inhibits Notch1 signaling in the developing *D. melanogaster* wing. Wing imaginal discs from 3rd instar larvae expressing *shSte14* in heat-shock induced clones marked with GFP and stained for Cut, a Notch-dependent gene product. (A) As described (41), cells stain for Cut in a band of 3-4 cells along the dorsal-ventral boundary of the disc. (B) Where the GFP positive clone intersects the line of Cut staining there is a decrease in the number of Cut positive cells (arrow). (C) A disc in which heat shock activated *UAS-shSte14* and GFP throughout the tissue shows no staining of Cut. Bar depicts 50 μm. See also Fig. S8D.

Supplemental Figure 8. Pharmacologic inhibition of Notch signaling blocks expression of p16^{INK4A} in cultured pancreatic ductal epithelial cells. PDECs harvested from wild-type mice were grown in 3D matrigel culture before shifting to 2D culture on plastic. Cells were treated with or without 1 μM of the γ secretase inhibitor compound E (CE) and analyzed on day 8 by immunoblot for Notch1, Delta4, β-tubulin and p16^{INK4A} as indicated. Results from the

quantification by Li-Cor Odyssey scanner of immunoblots from three independent experiments are plotted in the right panel (mean±SEM, normalized to control).

Supplemental Figure 9. Icmt deficiency enhances Wnt signaling. Immunohistochemical staining for β-catenin in paraffin sections of pancreata from 2 month old mice of the indicated genotypes imaged with 10x and 40x objectives. In the Icmt deficient pancreas there is an accumulation of cytoplasmic and nuclear β-catenin in PanIN lesions indicating enhanced Wnt signaling. Bars indicate 100 μm.

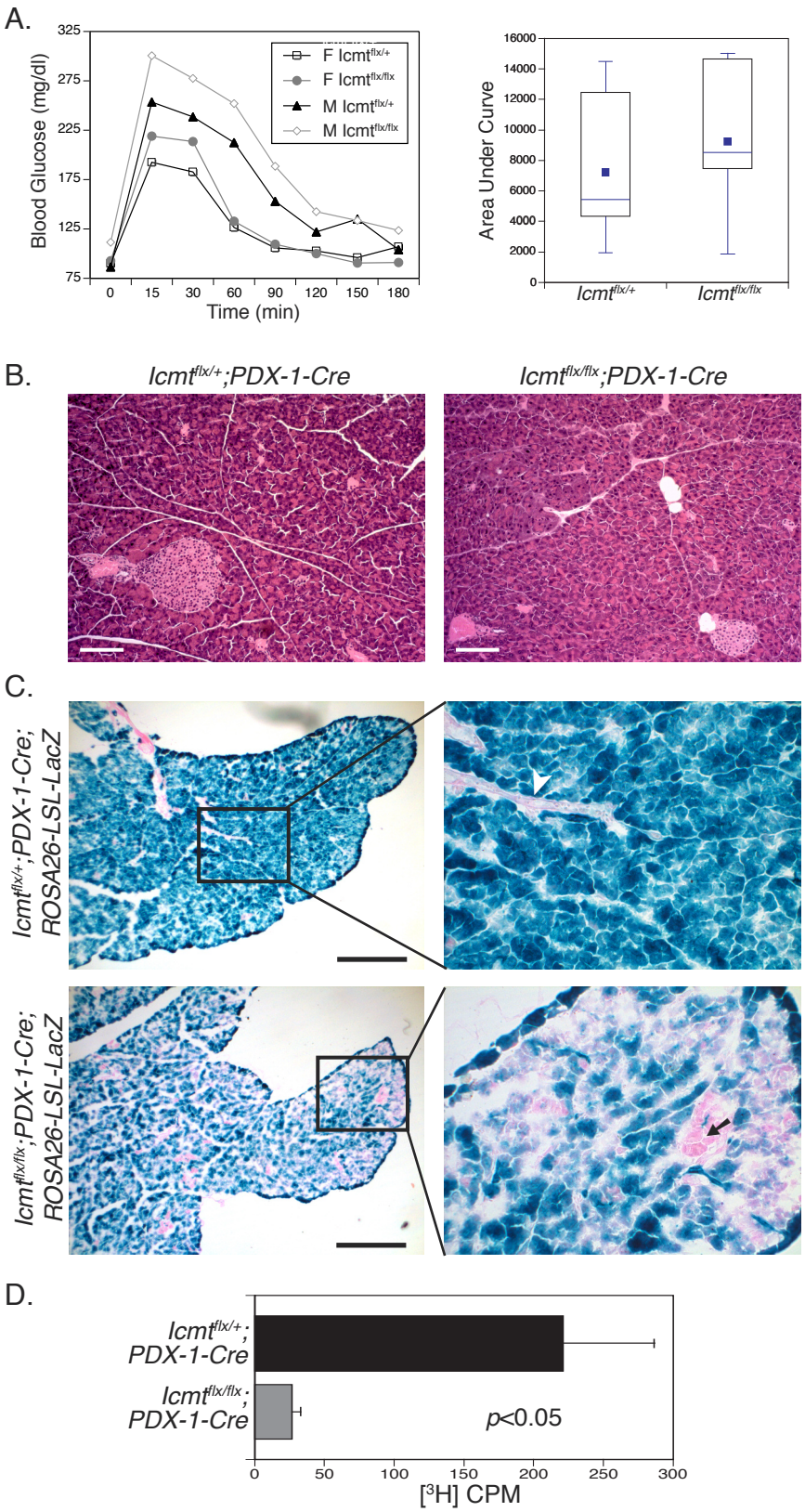
A.
Blood Glucose (mg/dl)
325
275
225
175
125
75
0
15
30
60
90
120
150
180
Time (min)
F Icmt flx/+
F Icmt flx/flx
M Icmt flx/+
M Icmt flx/flx
Area Under Curve
16000
14000
12000
10000
8000
6000
4000
2000
0
Icmt flx/+
Icmt flx/flx
B.
Icmt flx/+;PDX-1-Cre
Icmt flx/flx;PDX-1-Cre
C.
Icmt flx/+;PDX-1-Cre; ROSA26-LSL-LacZ
Icmt flx/flx;PDX-1-Cre; ROSA26-LSL-LacZ
D.
Icmt flx/+; PDX-1-Cre
Icmt flx/flx; PDX-1-Cre
p<0.05
0
50
100
150
200
250
300
[3H] CPM

Figure S1

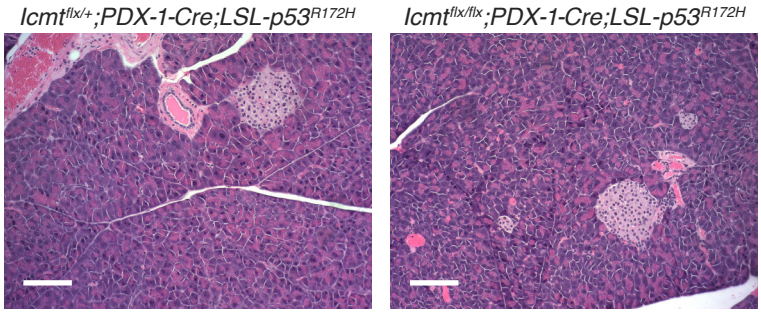
Icmt^flx/+;PDX-1-Cre;LSL-p53^R172H
Icmt^flx/flx;PDX-1-Cre;LSL-p53^R172H

Figure S2

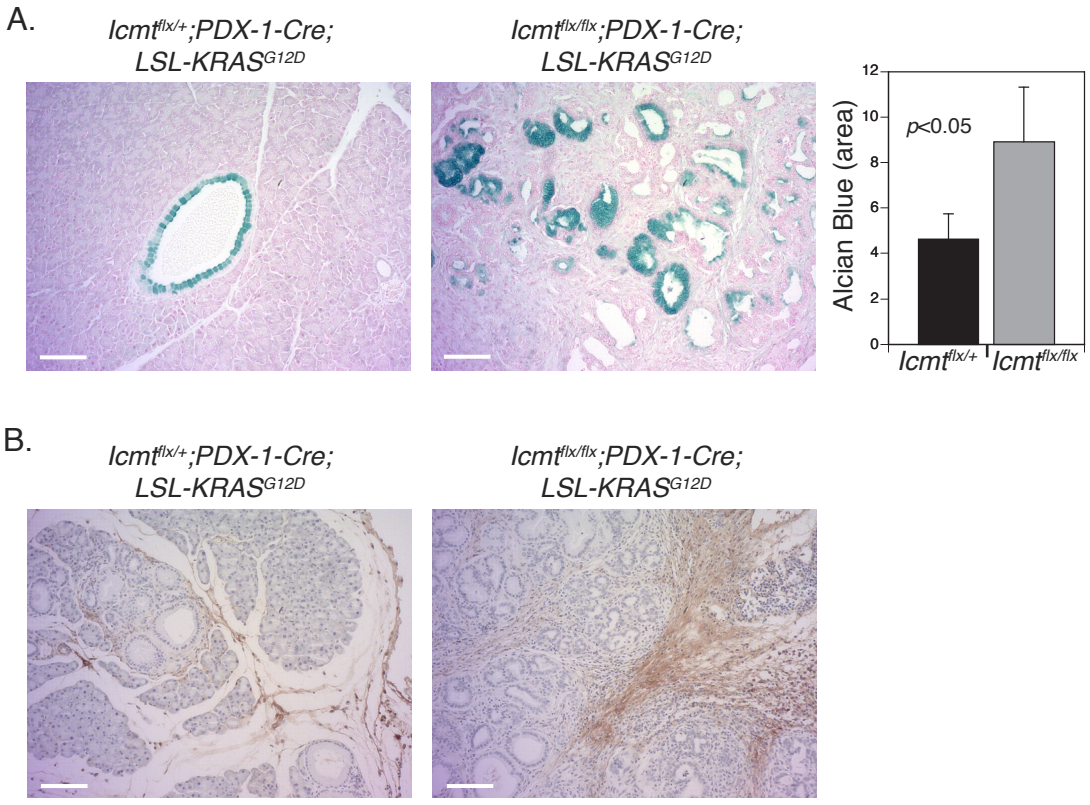
A.
Icmt^flx/+;PDX-1-Cre;
LSL-KRAS^G12D
Icmt^flx/flx;PDX-1-Cre;
LSL-KRAS^G12D
Alcian Blue (area)
p<0.05
0
2
4
6
8
10
12
Icmt^flx/+
Icmt^flx/flx
B.
Icmt^flx/+;PDX-1-Cre;
LSL-KRAS^G12D
Icmt^flx/flx;PDX-1-Cre;
LSL-KRAS^G12D

Figure S3

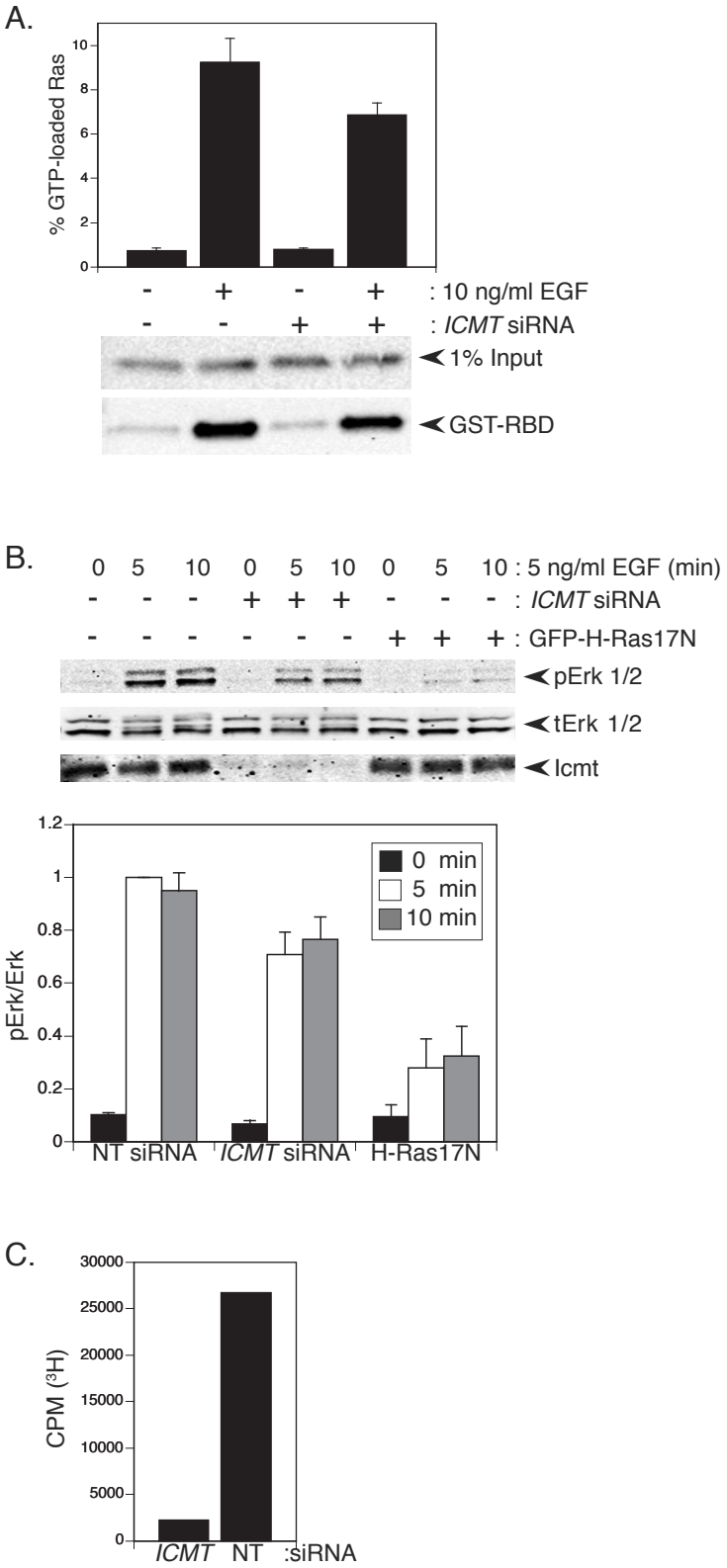
A.
% GTP-loaded Ras
10
8
6
4
2
0
- + - + : 10 ng/ml EGF
- - + + : ICMT siRNA
1% Input
GST-RBD
B.
0 5 10 0 5 10 0 5 10 : 5 ng/ml EGF (min)
- - - + + + - - - : ICMT siRNA
- - - - - - + + + : GFP-H-Ras17N
pErk 1/2
tErk 1/2
Icmt
pErk/Erk
1.2
1
0.8
0.6
0.4
0.2
0
0 min
5 min
10 min
NT siRNA
ICMT siRNA
H-Ras17N
C.
CPM (3H)
30000
25000
20000
15000
10000
5000
0
ICMT
NT
:siRNA

Figure S4

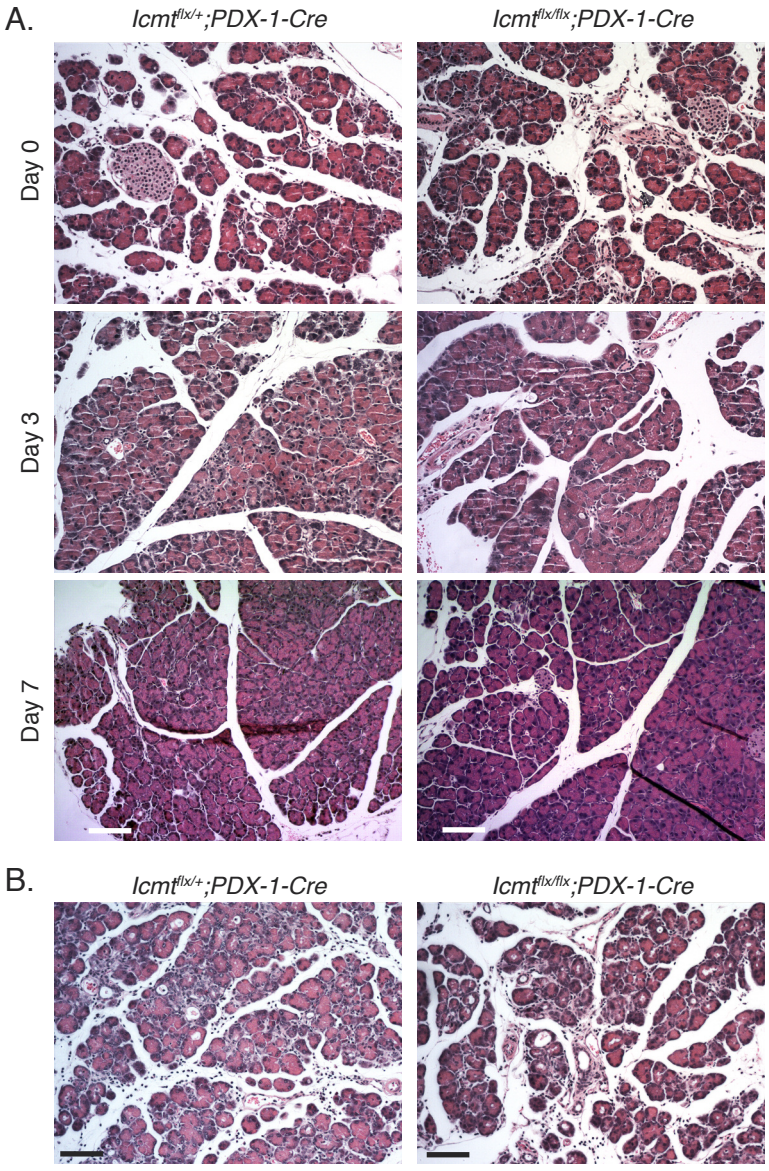
A.
Icmt^flx/+;PDX-1-Cre
Icmt^flx/flx;PDX-1-Cre
Day 0
Day 3
Day 7
B.
Icmt^flx/+;PDX-1-Cre
Icmt^flx/flx;PDX-1-Cre

Figure S5

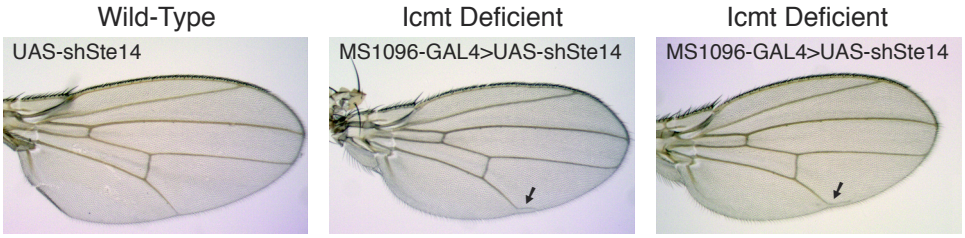
Wild-Type
Icmt Deficient
Icmt Deficient
UAS-shSte14
MS1096-GAL4>UAS-shSte14
MS1096-GAL4>UAS-shSte14

Figure S6

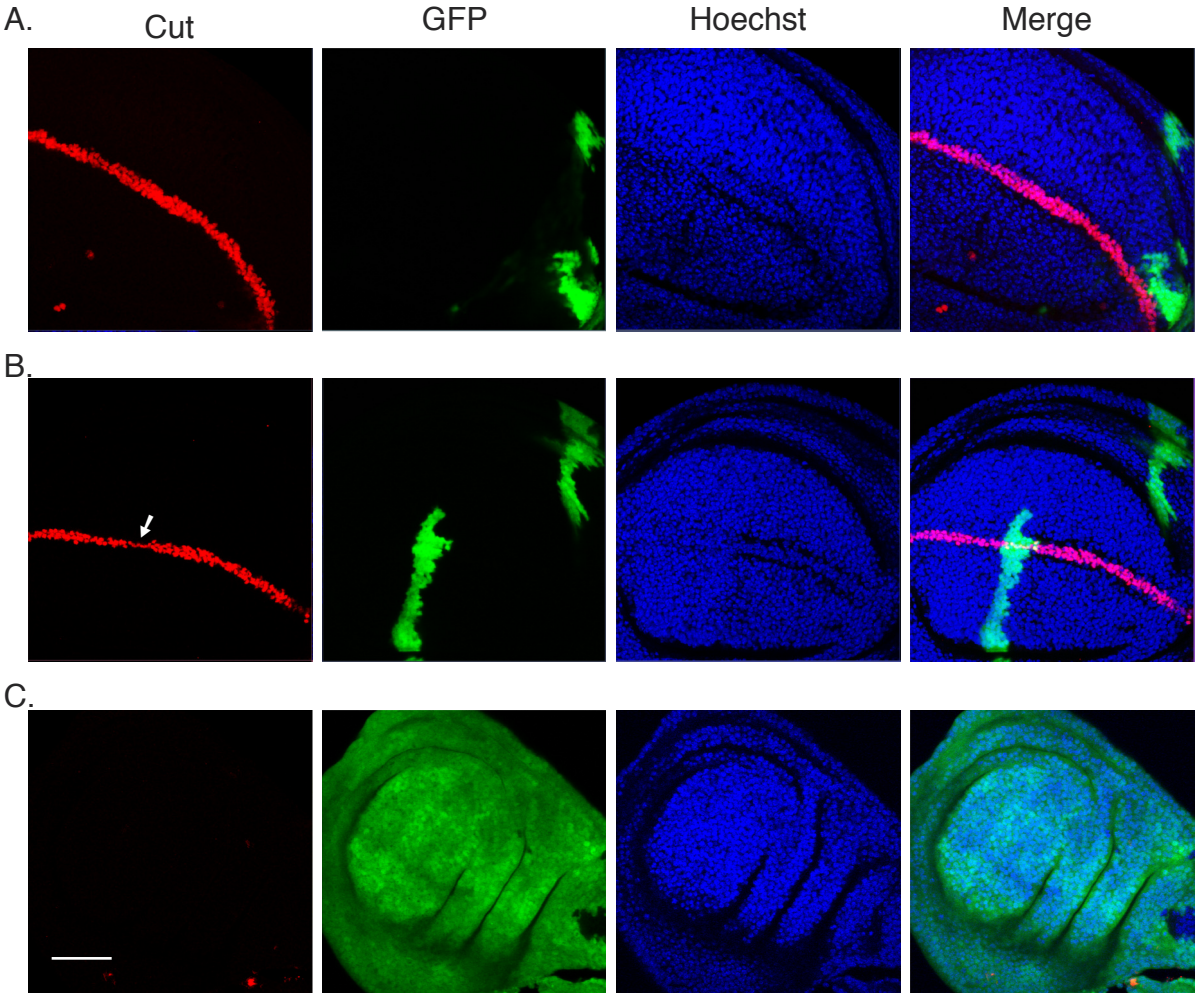

Figure S7

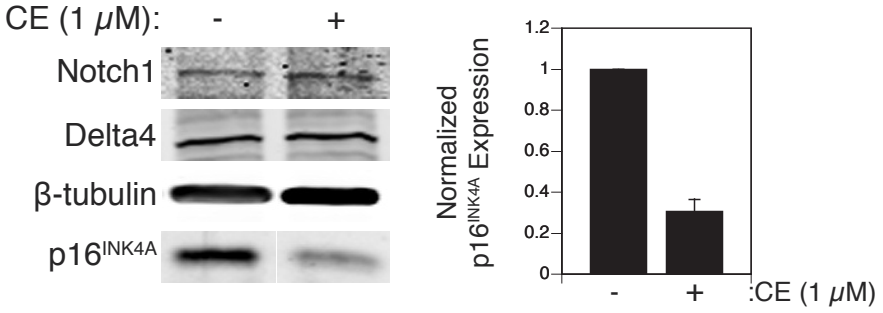
CE (1 μM): - +
Notch1
Delta4
β-tubulin
p16INK4A
Normalized p16INK4A Expression
1.2
1
0.8
0.6
0.4
0.2
0
- +
CE (1 μM)

Figure S8

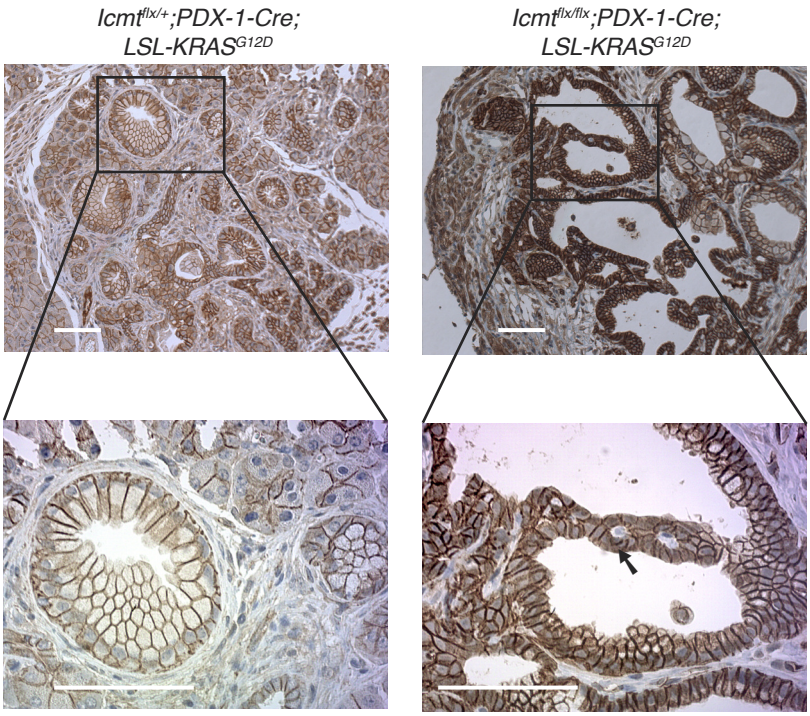
Icmt^flx/+;PDX-1-Cre;
LSL-KRAS^G12D
Icmt^flx/flx;PDX-1-Cre;
LSL-KRAS^G12D

Figure S9